

See discussions, stats, and author profiles for this publication at: <https://www.researchgate.net/publication/224206034>

A new single-phase PV fed five-level inverter topology connected to the grid

Conference Paper · November 2010

DOI: 10.1109/ICCCCT.2010.5670551 · Source: IEEE Xplore

CITATIONS

10

READS

249

3 authors, including:



Kaliamoorthy Mysamy

Dr. Mahalingam College of Engineering and Technology

22 PUBLICATIONS 158 CITATIONS

SEE PROFILE



Gerald Christopher Raj Irudayaraj

PSNACET

19 PUBLICATIONS 109 CITATIONS

SEE PROFILE

A new single-phase PV fed five-level inverter topology connected to the grid

M.Kaliamoorthy and R.M.Sekar

Assistant Professor

Department of Electrical and Electronics Engineering
PSNA College of Engineering and Technology
Dindigul, India

kalias_ifet@yahoo.com ssvedha08@gmail.com

I.Gerald Christopher Raj

Lecturer

Department of Electrical and Electronics Engineering
PSNA College of Engineering and Technology
Dindigul, India

gerald.gera@gmail.com

Abstract—There is a strong trend in the photovoltaic (PV) inverter technology to use transformerless topologies in order to acquire higher efficiencies. This paper presents a single-phase five-level grid connected PV inverter with a novel dual reference modulation technique. Two reference signals identical to each other with an offset equivalent to the amplitude of the rectified inverted sine carrier signal were used to generate PWM signals. The inverter consists of a full-bridge inverter and an auxiliary circuit comprising four diodes and a switch. The inverter produces output voltage in five levels: zero, $+1/2V_{dc}$, V_{dc} , $-1/2V_{dc}$ and $-V_{dc}$. The validity of the proposed inverter is verified through simulation.

Index Terms— PWM inverter, photovoltaic (PV), PI current control, grid-connected, multi-string.

I. INTRODUCTION

Nowadays, the main energy supplier of the worldwide economy is fossil fuel. This however has led to many problems such as global warming and air pollution. Therefore, with regard to the worldwide trend of green energy, solar power technology has become one of the most promising energy resources. The number of PV installations has had an exponential growth [1]. One of the most important types of PV installation is the grid connected inverter configurations. These grid connected PV systems can be categorized from two viewpoints: PV cell and inverter configurations. The PV cell arrangements fall into four broad groups: centralized technology, string technology, multi-string technology and AC-module and AC-cell technologies [2].

All approaches have advantages and disadvantages [2], [3]; and will compromise various attributes such as harmonic generation, complexity, efficiency, flexibility, reliability, safety, modularity and cost. However, for residential PV installations, the most suitable configuration seems to be the string or multi string technologies where one or more strings of PV cells are connected to a single inverter. Using this type of configuration, there will be no losses associated with the string diodes compared to centralized technology. Moreover, independent Maximum Power Point Tracking (MPPT) is possible for all strings which might be installed in different sizes and orientations. This also increases the overall efficiency under special circumstances like partial shadowing.

There are different approaches to implement string and multi-string topologies. Usually, these modules consist of a solar array and a DC to DC converter controlled by a MPPT algorithm. Afterwards, the outputs of the DC/DC converters build up a DC voltage which is then converted to AC by means of an inverter [4]. The other possibility is to use multilevel. PV systems categorized by different PV cell configurations and inverter types topologies which are able to generate better output quality, while operating at lower switching frequency. This implies lower switching dissipation and higher efficiency. Moreover, this topology utilizes switches with lower breakdown voltage; therefore, it can be used in higher power applications at lower cost. It is worth mentioning that although the number of switches in this approach is higher than other two level topologies, for a sufficient high number of levels, the output filter can be avoided which means less weight, cost and space.

This paper presents a single-phase five-level inverter with a transformer for grid-connected application. A five-level configuration is used because it offers great advantages such as improved output waveforms, smaller filter size, lower EMI and lower THD compared with conventional three-level PWM inverter [2]-[3]. To generate output voltage in five-levels, full bridge inverter configuration together with an auxiliary circuit as shown in Fig. 1 were used.

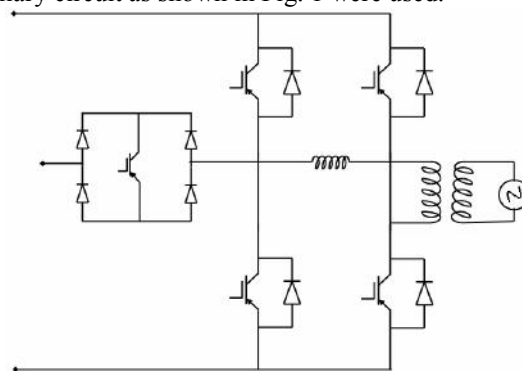


Fig 1 Five Level Inverter with an Auxiliary Switch

Dual reference modulation technique is introduced to generate switching signals for the switches and to produce five output voltage levels: zero, $+1/2V_{dc}$, V_{dc} , $-1/2V_{dc}$ and $-V_{dc}$ (assuming V_{dc} is the supply voltage). The modulating

technique uses two reference signals instead of one to generate PWM signals for the switches. Both the reference signals Vref1 and Vref2 are identical to each other except for an offset value equivalent to the amplitude of the carrier signal Vcarrier as shown in Fig. 2.

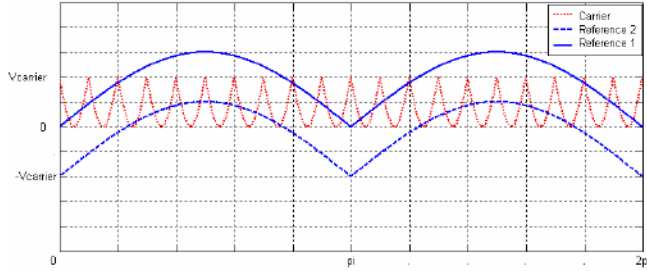


Fig 2 Carrier and Reference Signals

II. PV PANEL MODELING

The possibility of predicting a photovoltaic plant's behavior in variance irradiance and temperature is very important for sizing the PV plant and converter. There are numerous methods presented in the literature, for extracting the panel parameters. In this paper a photovoltaic panel model based on the manufacturer's data sheet is presented. The equivalent circuit of the single-diode model for the PV cells is shown in fig 3 [9]. Series resistance (R_s) and shunt resistance (R_{SH}) are parasitic resistances. In this model the effect of R_{SH} is neglected to simplify the model. The output voltage of the PV cell is given by:

$$V_c = \frac{AkT_c}{e} \ln \left[\frac{I_{ph} + I_0 - I_c}{I_0} \right] - R_s I_c \quad (1)$$

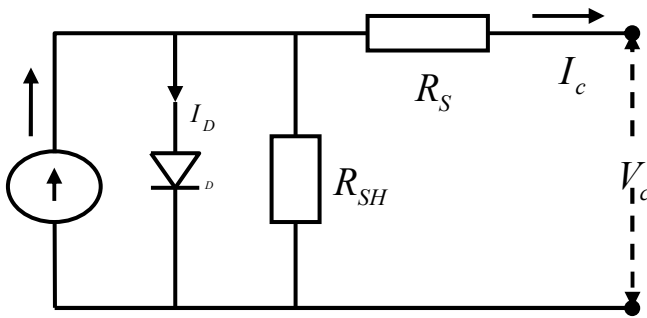


Fig 3 Equivalent Circuit of PV Cell

Active compensation of series resistance, cell output voltage and photo current are taken into account in the modeling of solar PV panel. R_s , V_c , I_{ph} are taken as a function of temperature and irradiance. Thermal voltage for variable temperature T_x

$$V_t = \frac{A_D k T_n c}{e} \quad (2)$$

Diode ideality factor:

$$A_D = \frac{-(I_{mpp} - I_{sc}) * V_{mpp}}{V_t * I_{mpp}} \quad (3)$$

Series resistance calculation using datasheet values:

$$R_s = -V_{mpp} - \ln \left[\frac{-I_{mpp} + I_{sc}}{I_{sc}} \right] \left[\frac{I_{mpp} - I_{sc}}{I_{mpp}} \right] \frac{V_{mpp}}{V_{oc}} + V_{oc} \quad (4)$$

Open circuit voltage:

$$V_{oc} = \ln \left[\frac{I_{sc}}{I_0} \right] V_t \quad (5)$$

Temperature dependence of voltage:

$$V_{ocT} = V_{oc} + K_v (T_x - T_c) \quad (6)$$

The short circuit current and photo current were considered to be proportional to the value of irradiation:

$$I_{scG} = I_{sc} S_x \quad (7)$$

$$I_{phG} = I_{ph} S_x \quad (8)$$

Dark saturation current:

$$I_0 = \frac{-I_{scT}}{\frac{V_{oc}}{V_t} + e^{\frac{I_{scT} R_s}{V_t}} - 0.001} \quad (9)$$

The output voltage of the PV panel, compensated for irradiance and temperature:

$$V_x = \frac{-I_x R_s + \ln \left[-I_x e^{\frac{V_{oc}}{V_t}} - I_x e^{\frac{I_{scT} R_s}{V_t}} - I_{sc} e^{\frac{V_{oc}}{V_t}} \right]}{I_{sc}} \quad (10)$$

PV current compensated for irradiance and temperature:

$$I_x = I_{scT} S_x \quad (11)$$

III. PV MODULE SIMULATION RESULTS

The photovoltaic module was simulated using MATLAB/SIMULINK. The parameters of the photovoltaic cell used for the simulation is given in the table I.

$I_{sc, ref}$	2.664 A
R_s	1.324 Ω
$V_{oc, ref}$	87.72 V
$V_{mpp, ref}$	70.731 V
$I_{mpp, ref}$	2.448 A
S_x	1000 W/m ²
T_c	25°C
K_v	5x10 ⁴ J/(°C.m ²)
A	1.5 m ²

Table I PV Module Parameters

The simulation is carried out for the above mentioned parameters for constant irradiance and constant cell temperature. Figure 4 shows the VI characteristics of the photovoltaic cell for constant irradiance and Figure 5 shows the PV Characteristics of photovoltaic cell at constant irradiance. It can be observed from the figure 4 and 5 that the maximum power point of the photovoltaic cell varies for all different conditions.

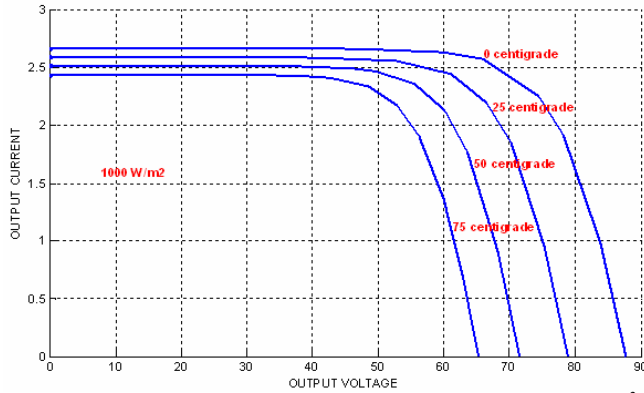
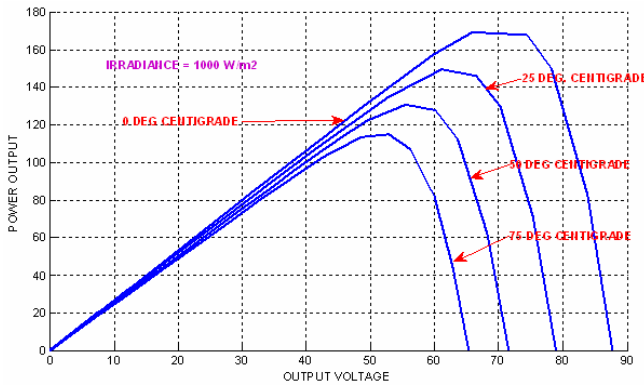
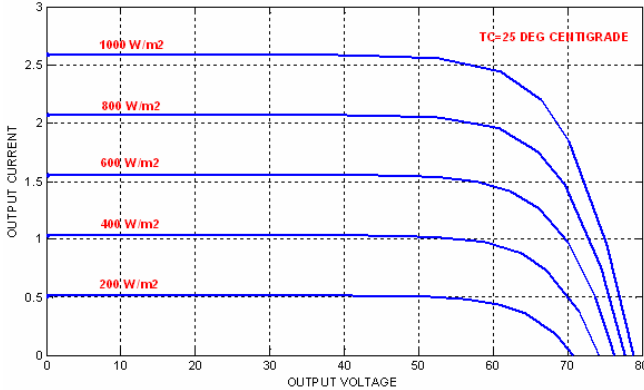

 Fig 4 VI Characteristics of PV cell for constant irradiance of 1000 W/m²

 Fig 5 PV Characteristics of PV cell for constant irradiance of 1000 W/m²


Fig 6 VI Characteristics of PV cell for constant cell temperature of 25°C

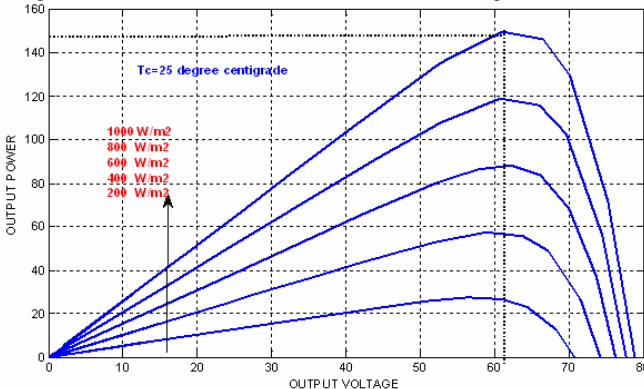


Fig 7 PV Characteristics of PV cell for constant cell temperature of 25°C

Similarly figure 6 and figure 7 shows VI characteristics and PV characteristics of photovoltaic cell at constant cell temperature. These figures also show that the maximum power point (MPP) varies for all the different irradiance.

IV. FIVE LEVEL INVERTER TOPOLOGY

The proposed single-phase five-level inverter topology is shown in Fig. 4. It consists of a dc-dc boost converter connected to two capacitors in series, an auxiliary circuit, a full-bridge a full-bridge inverter, a step-up transformer and utility grid. In this paper, the inverter is designed to work as a grid connected system; therefore utility grid is used instead of load. The dc-dc boost converters are used to track the maximum power point (MPP) of the solar arrays as well as to step-up the inverter output voltage V_{inv} to be more than $\sqrt{2}$ of the grid voltage V_g to ensure power flow from the PV arrays into the grid. As a step-up transformer with a ratio of 1:2 is used V_{inv} should be

$$V_{inv} > \frac{\sqrt{2}V_g}{2} \quad (12) \text{ (Or)}$$

$$V_{inv} > \frac{V_g}{\sqrt{2}} \quad (13)$$

A filtering inductance L_f is used to filter the current injected into the grid. The injected current must be sinusoidal with low harmonic distortion [8]. The flowchart of the Maximum Power Point Tracking algorithm is shown in the figure 8.

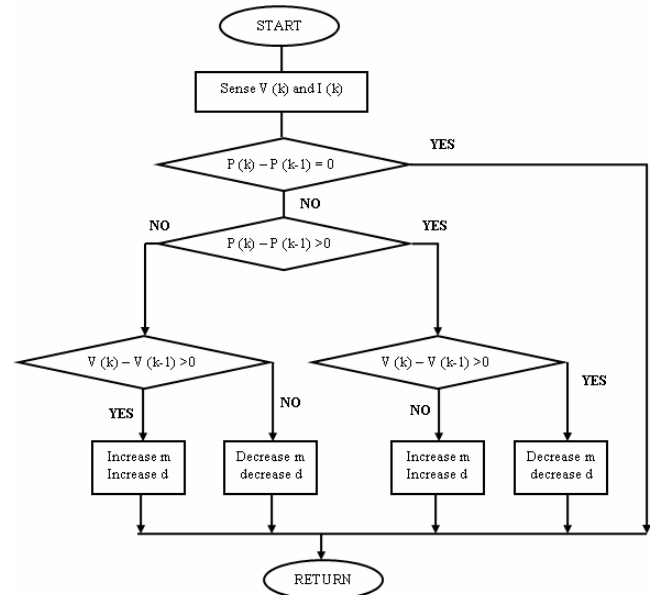


Fig 8 Flowchart for Maximum Power Point Tracking algorithm (MPPT)

The results of the MPPT algorithm are shown in the figure 9 and figure 10. It is evident from the figures that the algorithm is tracking the maximum power efficiently at all the operating points. This algorithm is also known as perturb and observe algorithm.

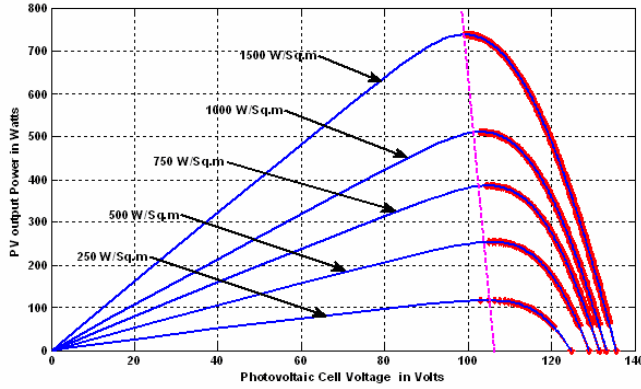


Fig 9 PV characteristics of photovoltaic cell after MPPT algorithm

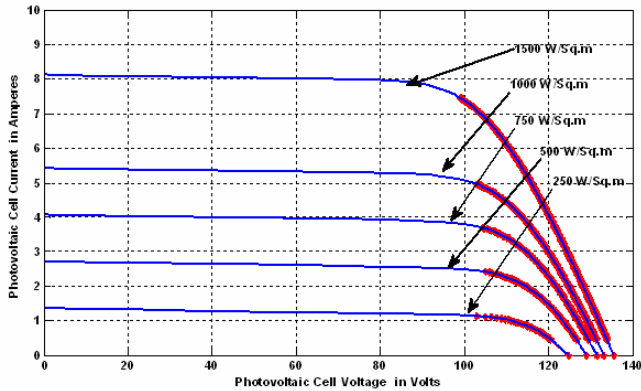


Fig 10 VI characteristics of photovoltaic cell after MPPT algorithm

V. PWM STATERGY AND OPERATING PRINCIPLE

Modulation index M_a for five-level PWM inverter is given as [9]

$$M_a = \frac{A_m}{2A_c} \quad (14)$$

Where A_c is the peak-to-peak value of carrier and A_m is the peak value of voltage reference V_{ref} . Since in this work two reference signals identical to each other are used, equation (14) can be expressed in terms of amplitude of carrier signal V_c by replacing A_c with V_c . and $A_m = V_{ref1} = V_{ref2} = V_{ref}$.

$$M = \frac{V_{ref}}{2V_c} \quad (15)$$

If $M > 1$, higher harmonics in the phase waveform is obtained. Therefore, M is maintained between 0 and 1. If the amplitude of the reference signal is increased higher than the amplitude of the carrier signal, i.e. $M > 1$, this will lead to over modulation. Large values of M in sinusoidal PWM techniques lead to full over modulation [10].

From the PWM modulation, the analysis of harmonic components in the proposed inverter can be preformed. The output voltage produced by comparison of the two reference signals and the carrier signal can be expressed as [3].

$$V_a(\theta) = A_0 + \sum_{n=1}^{\infty} (A_n \cos n\theta + B_n \sin n\theta) \quad (16)$$

If there are P pulses per quarter period, and it is an odd number, the coefficients B_n and A_0 would be a zero where n is an even number. Therefore, the equation (16) can be rewritten as

$$V_a(\theta) = \sum_{n=1,3,5,\dots}^{\infty} A_n \cos n\theta \quad (17)$$

$$A_n = -\frac{2V_{dc}}{n\pi} \sum_{m=0}^P \sum_{i=1}^4 \left[(-1)^{\text{int}(i/2)} \sin(n\alpha_{m+i}) \right] \quad (18)$$

Where m is the pulse number. The Fourier series coefficients of the conventional single-phase full-bridge inverter by sinusoidal PWM is given as

$$A_n = \frac{4V_{dc}}{n\pi} \sum_{m=1}^P \left[(-1)^m \sin(n\alpha_m) \right] \quad (19)$$

The main objective of designing a grid-connected PV inverter is to inject sinusoidal current into the utility grid. In order to generate sinusoidal current with low harmonic distortion, a sinusoidal PWM is used since it is one of the most effective methods. Sinusoidal PWM is obtained by comparing a high-frequency carrier with a low-frequency sinusoid, which is the modulating signal or reference signal. The carrier has a constant period; therefore, the switches have constant switching frequency. The switching instant is determined from the crossing of the carrier and the modulating signal.

In this paper, a dual reference modulation technique is incorporated into the sinusoidal PWM technique to produce PWM switching signals for the full-bridge inverter switches and auxiliary switch. Two reference signals V_{ref1} and V_{ref2} will take turns to be compared to the carrier signal at a time. If V_{ref1} exceeds the peak amplitude of the carrier signal $V_{carrier}$, then V_{ref2} will be compared to the carrier signal until it reaches 0. At this point onward, V_{ref1} takes over the comparison process until it exceeds $V_{carrier}$. This will lead to a switching pattern, as shown in 11.

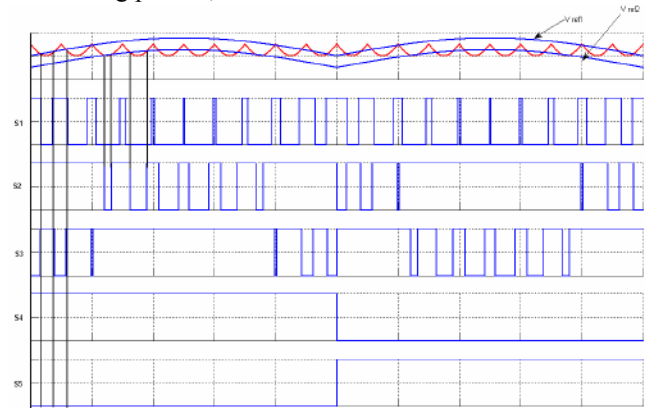


Fig. 11. Switching pattern for single-phase five-level inverter.

Switches S_2 – S_4 will be switching at the rate of the carrier signal frequency, while S_5 and S_6 will operate at a frequency equivalent to the fundamental frequency. Table II illustrates the level of V_{inv} during S_2 – S_6 switch on and off.

S ₂	S ₃	S ₄	S ₅	S ₆	V _{INV}
ON	OFF	OFF	OFF	ON	$+V_{pv}/2$
OFF	ON	OFF	OFF	ON	$+V_{pv}$
OFF	OFF or ON	OFF or ON	ON or OFF	ON or OFF	0
OFF	OFF	OFF	ON	OFF	$-V_{pv}/2$
OFF	OFF	ON	ON	OFF	$-V_{pv}$

 TABLE II. Inverter output voltage during S₂–S₆ switch on and off.

V. CLOSED LOOP CONTROL SYSTEM

The proposed inverter is used in a grid-connected PV system. Therefore, a PI current control scheme is employed to keep the output current sinusoidal and to have high dynamic performance under rapidly changing atmospheric conditions and to maintain the power factor at near unity. As the irradiance level is inconsistent throughout the day, the amount of electric power generated by the solar modules is always changing with weather conditions. To overcome this problem, Maximum Power Point Tracking (MPPT) algorithm is used. It tracks the operating point of the I-V curve to its maximum value. Therefore, the MPPT algorithm will ensure maximum power is delivered from the solar modules at any particular weather conditions. Various MPPT control algorithm have been discussed in detail in [11]-[13].

In this proposed inverter, Perturb and Observe (P&O) algorithm is used to extract maximum power from the PV modules. The feedback PI current control senses the current injected into the grid also known as grid current I_g and feed back to a comparator which compares it with reference current I_{ref} . I_{ref} is obtained by sensing the grid voltage and converting it to reference current and multiplying it with variable m . Variable m is derived from the MPPT algorithm as illustrated in the flowchart in Fig. 8. The five-level inverter with the control algorithm used in simulation environment is shown in Fig. 12. Since variable m and D is dependent on the MPPT algorithm, as the irradiance level increases, variable m also increases. Therefore it can be concluded that,

$$M, D \propto \text{irradiance of the sun}$$

The instantaneous current error from the comparison between I_{ref} and I_g is fed to a PI controller. The integral term in the PI controller improves the tracking by reducing the instantaneous error between the reference and the actual current. The resulting error signal u which forms the dual reference signals V_{ref1} and V_{ref2} is compared with a rectified inverted sine carrier signal and intersections are sought to produce PWM signals for the inverter switches. This is to ensure I_g to be in phase with grid voltage V_g and always at near unity power factor.

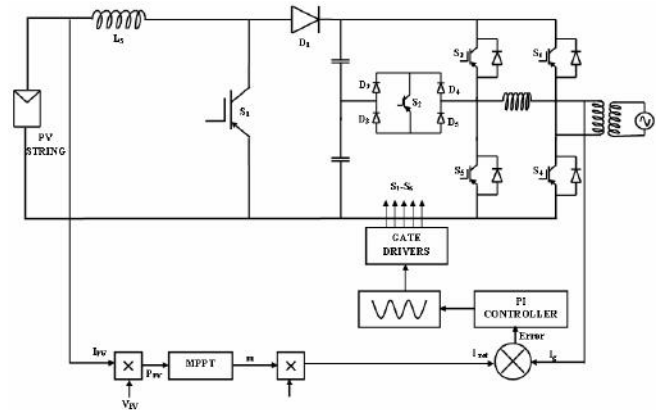


Fig 12 Closed Loop Block Diagram of grid connected five level inverter.

VI. SIMULATION RESULTS.

Simulations were performed by using MATLAB SIMULINK to verify that the proposed inverter can be practically implemented in a PV system. It helps to confirm the PWM switching strategy for the five-level inverter. Then, Fig. 13(a) shows the way the PWM switching signals are generated by using two reference signals and a triangular carrier signal. The resulting PWM signals for switches S2 to S6 are shown in Fig. 13 (b)-(f). Note that one leg of the inverter is operating at a high switching rate equivalent to the frequency of the carrier signal while the other leg is operating at the rate of fundamental frequency (i.e. 50Hz). The switch at the auxiliary circuit S2 also operates at the rate of the carrier signal. As mentioned earlier, the modulation index M will determine the shape of the inverter output voltage V_{inv} and the grid current I_g . Fig. 14 shows simulation results of V_{inv} and I_g for different values of M and D .

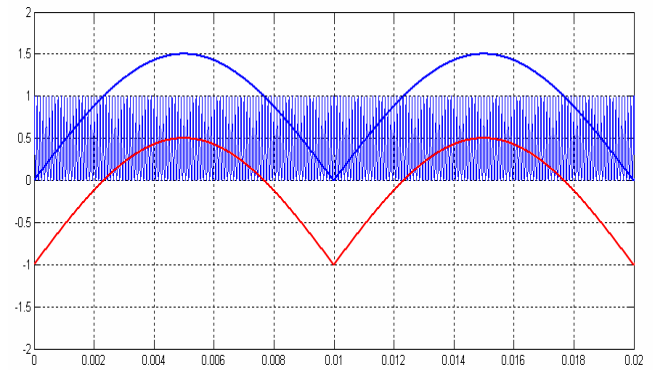
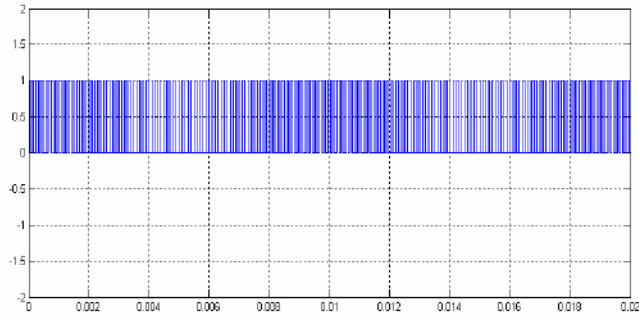
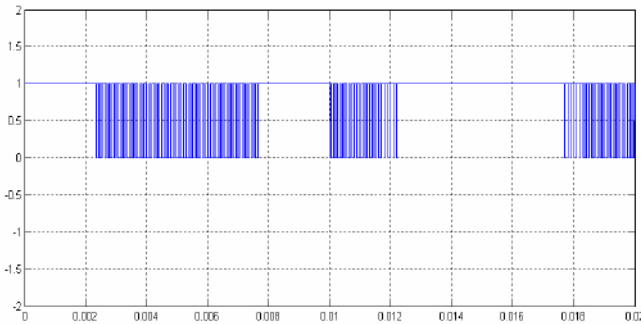
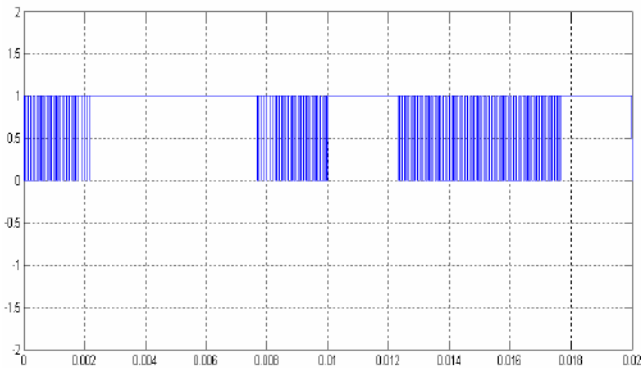
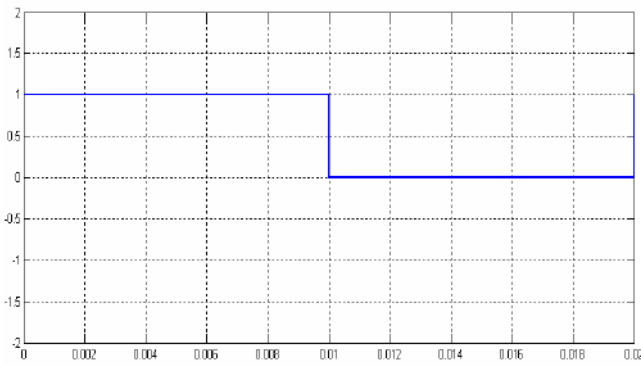
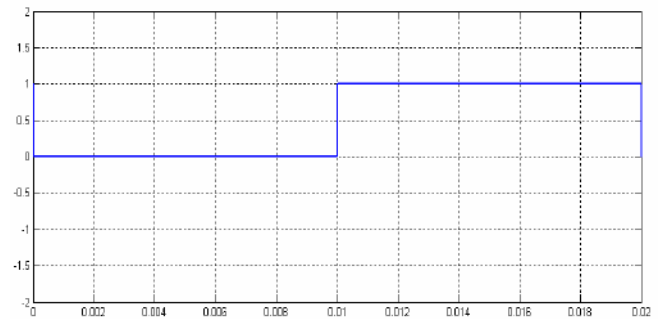
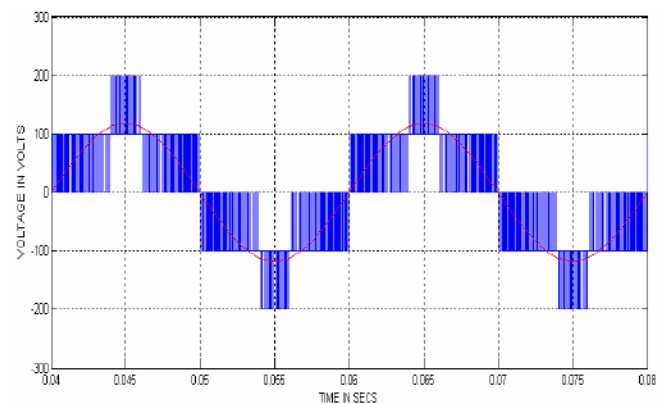
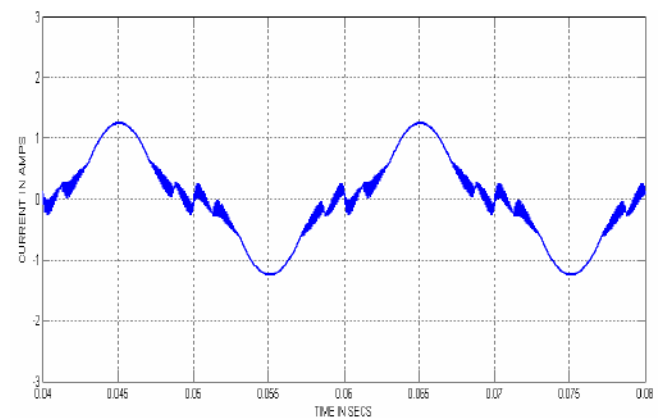


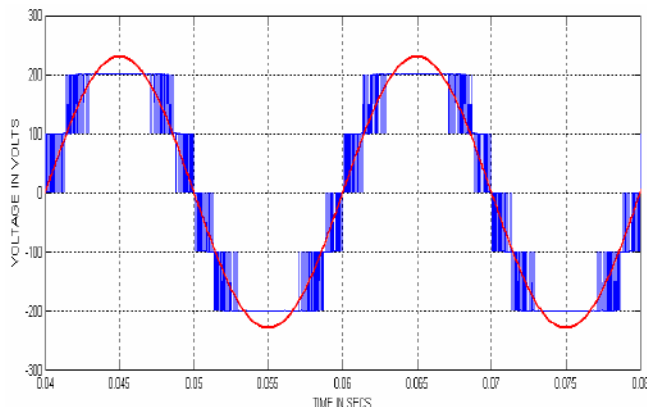
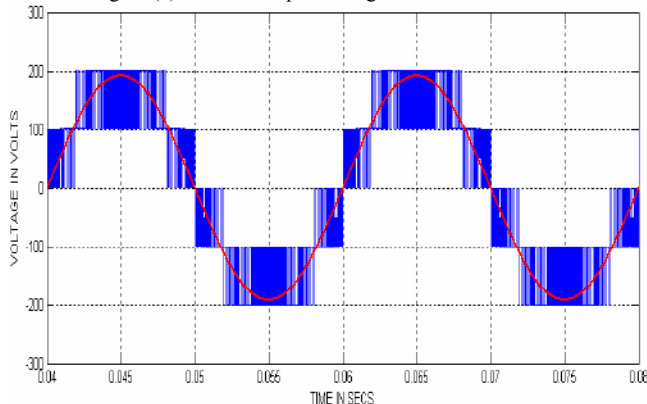
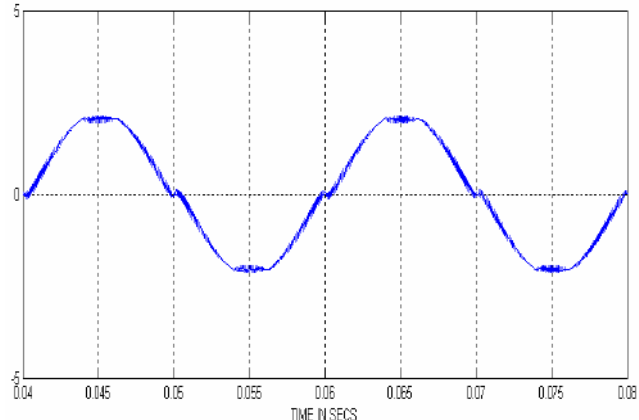
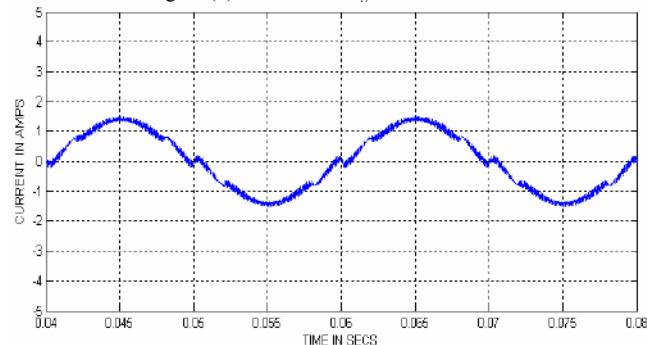
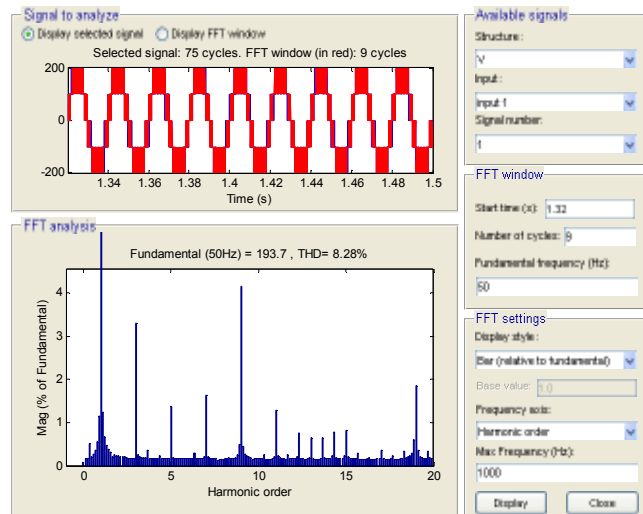
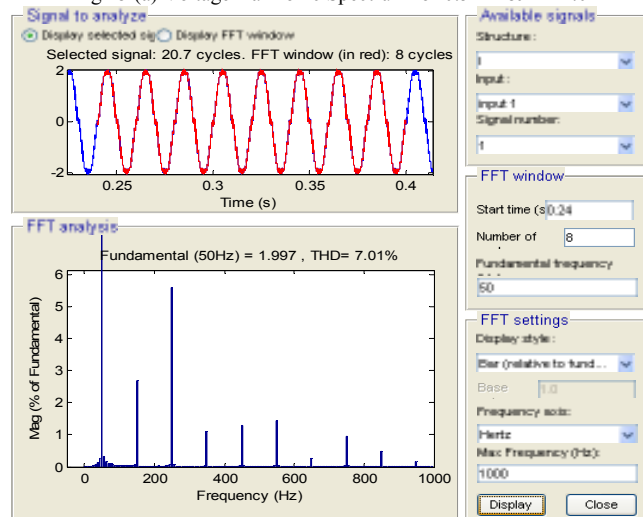
Fig 13 (a) PWM Signal Generation

Referring to equations (12) and (13), the dc bus voltage is set to 200V ($> V_g / \sqrt{2}$, in this case V_g is 240V) to inject current into the grid. Fig. 14(a) shows V_{inv} is less than $V_g / \sqrt{2}$ due to M being less than 0.5. The inverter should not operate at this condition because the current will be injected from the grid into the inverter as shown in Fig. 14(b).


 Fig 13 (b) PWM Switching Signal to S_2

 Fig 13 (c) PWM Switching Signal to S_3

 Fig 13 (d) PWM Switching Signal to S_4

 Fig 13 (e) PWM Switching Signal to S_5

 Fig 13 (f) PWM Switching Signal to S_6

Over modulation condition, which happens when $M > 1.0$, is shown in Fig. 14 (c). It has a flat top at the peak of the positive and the negative cycles because both the reference signals exceed the maximum amplitude of the carrier signal. This will cause I_g to have a flat portion at the peak of the sine waveform as shown in Fig 14 (d). To optimize the power transferred from the PV arrays to the grid, it is recommended to operate at $0.5 \leq M \leq 1.0$. V_{inv} and I_g for optimal operating condition are shown in Fig. 14 (e) and (f). As I_g is almost a pure sine wave, the total harmonic distortion (THD) can be reduced compared with that under other values of M .


 Fig 14 (a) Inverter Output Voltage V_{inv} for M & $D < 0.5$

 Fig 14 (b) Grid Current I_g for M & $D < 0.5$


 Fig 14 (c) Inverter Output Voltage V_{inv} for $M \& D > 1.0$

 Fig 14 (e) Inverter Output Voltage V_{inv} for $0.5 < M \& D < 1.0$

 Fig 14 (d) Grid Current I_g for $M \& D > 1.0$

 Fig 14 (f) Grid Current I_g for $0.5 < M \& D < 1.0$

 Fig 15 (a) Voltage Harmonic Spectrum for $0.5 < M \& D < 1.0$

 Fig 15 (b) Current Harmonic Spectrum for $0.5 < M \& D < 1.0$

VII. CONCLUSION

This paper presented a single-phase five-level inverter with a dual reference modulation technique for PV application. The dual reference modulation technique involves comparing two reference signals identical to each other except for an offset equivalent to its carrier signal, with a rectified inverted sine carrier signal to generate PWM switching signals for the switches. The circuit topology, control algorithm and operational principle of the proposed inverter were analyzed in detail. The results show that the THD of the five-level inverter is much less than that of the conventional three-level inverter. Furthermore, both the grid voltage and the grid current are in phase at near unity power factor.

REFERENCES

- [1] N. A. Rahim, Saad Mekhilef, "Implementation of Three Phase grid Connected Inverter for Photovoltaic Solar Power Generation System" Proceedings IEEE. Power Con 2002. Vol 1, pp. 570 – 573, Oct 2002.

- [2] S.. Kouro, J.. Rebollo, J. Rodriguez, "Reduced Switching-Frequency-Modulation Algorithm for High-Power Multilevel Inverters," IEEE Trans. on Industrial Electronics, vol. 54, no. 5, pp. 2894-2901, Oct. 2007.
- [3] S. J. Park, F. S. Kang, M. H. Lee, C. U. Kim, "A New Single-Phase Five-Level PWM Inverter Employing a Deadbeat Control Scheme," IEEE Trans. Power Electronics., vol. 18, no. 18, pp. 831-843, May. 2003.
- [4] L. M. Tolbert, T. G. Habetler, "Novel Multilevel Inverter Carrier-Based PWM Method," IEEE Trans. Industry Application., vol. 35, no.5, pp. 1098-1107, Sept/Oct 1999.
- [5] M. Calais, L. J. Borle, V. G. Agelidis, "Analysis of Multicarrier PWM Methods for a Single-Phase Five-Level Inverter," Power Electronics Specialists Conference 2001. PESC 01. 2001 IEEE 32th Annual Volume 3, 17-21 June 2001 pp: 1173 - 1178 Vol.3,.
- [6] N. S. Choi, J. G. Cho, G. H. Cho, "A General Circuit Topology of Multilevel Inverter," Power Electronics Specialists Conference, 1991. PESC' 91. 1991 IEEE 22th Annual Volume, 24-27 June 1991 pp. 96 – 103.
- [7] G. Carrara, S. Gardella, M. Marchesoni, R. Salutati, G. Sciutto, "A New Multilevel PWM method: A Theoretical Analysis," IEEE Trans. Power Electronics., vol. 7, no. 3, pp. 497 - 505, July. 1992.
- [8] V. G. Agelidis, D. M. Baker, W. B. Lawrance, C. V. Nayar, "A Multilevel PWM Inverter Topology for Photovoltaic Application," in Proc. IEEE ISIE'97, Guimaraes, Portugal, 1997, pp. 589-594.
- [9] Muhammad H. Rashid, Power electronics: Circuits, Devices, and Applications, 3rd ed. Pearson Prentice Hall, 2004, pp.267.
- [10] Eram T, Chapman P.L, "Comparison of Photovoltaic Array Maximum Power Point Tracking Techniques," IEEE Trans. Energy Conversion, vol. 22, no. 2, pp. 439- 449, June 2007.
- [11] Femia N., Petrone G., Spagnuolo G., Vitelli M: "Optimizing duty-cycle perturbation of P&O MPPT technique" Power Electronics Specialists Conference, 2004. PESC 04. 2004 IEEE 35th Annual Volume 3, 20- 25 June 2004 pp. 1939 - 1944 Vol.3
- [12] Liu X., Lopes L.A.C.: "An improved perturbation and observation maximum power point tracking algorithm for PV arrays" Power Electronics Specialists Conference, 2004. PESC 04. 2004 IEEE 35th Annual Volume 3, 20-25 June 2004 pp. 2005 - 2010 Vol.3.



M.Kaliamoorthy received the M.Tech degree in electrical drives and control from Pondicherry University, India, in 2006. He is currently working as an assistant professor in PSNA College of Engineering and technology, Dindigul, Tamilnadu, India in the Department of Electrical and Electronics Engineering. His research interests include alternative energy sources, fuel cells, energy conversion, power system modeling, analysis and control, power quality and active harmonic analysis.



R.M.Sekar received the M.Tech degree in Power Electronics from VIT University, India, in 2004. He is currently working as an assistant professor in PSNA College of Engineering and technology, Dindigul, Tamilnadu, India in the Department of Electrical and Electronics Engineering. His research interests include multilevel inverters, alternative energy sources, energy conversion, power quality, active harmonic analysis and Facts devices analysis and control.



I.Gerald Christopher Raj received the M.E degree in Power Electronics and drives from Anna University, India, in 2006. He is currently working as an Lecturer in PSNA College of Engineering and technology, Dindigul, Tamilnadu, India in the Department of Electrical and Electronics Engineering. His research interests include CSI fed AC motor drives, energy conversion, power system modeling, analysis and control and power quality